

Enhancing Natural BChl *a* Adsorption Capacity and Photoelectric Performance of BChl *a*-based DSSC by Improving TiO₂ Photoanode

Xiaobo Zhang¹, Xixiang Xiao^{1,2}, Bitong Zhu¹, Chungui Zhao^{1,*}, Suping Yang^{1,*},
Qiaoming Fu¹

¹ College of Chemical Engineering, Huaqiao University, Xiamen 361021, China

² College of Ecological Environment and Urban Construction, Fujian University of Technology, Fuzhou 350118, China.

*E-mail: chungui@hqu.edu.cn; yangsuping@hqu.edu.cn

Received: 10 March 2018 / Accepted: 9 May 2018 / Published: 5 June 2018

Natural bacteriochlorophyll (BChl) *a* from purple bacteria possesses the near-infrared absorption, high extinction coefficient and excellent photoelectric properties. It is a promising natural pigment sensitizer candidate for fabricating near-infrared responsive dye-sensitized solar cell (DSSC). However, its low adsorption capacity on TiO₂ film limited its photoelectric performance. To enhance adsorption capacity of BChl *a* on the electrode, in this study, the TiCl₄ and acetic acid treatment were used to modify the TiO₂ film (named as T-TiO₂ film and A-TiO₂ film, respectively). The optimal adsorption parameters were examined by adsorption kinetic and adsorption isotherms of BChl *a* on the different types of TiO₂ films. The effects of TiO₂ film thickness and pigment concentrations on adsorption capacity and photoelectric properties of BChl *a* were systematically investigated. The results showed that T-TiO₂ film achieved the maximum adsorption capacity and adsorption rate for BChl *a*, the adsorption capacity of BChl *a* was increased gradually with increasing TiO₂ film thickness, but the best photoelectric performance was obtained at the moderate film thickness of 10 μm and 480 μg·ml⁻¹ of BChl *a*. The maximum short-circuits current and photoelectric conversion efficiency of DSSC obtained were 3.51 mA·cm⁻² and 1.67% at 100 mW·cm⁻², which were eight times and fifteen times higher than those of untreated TiO₂ films with thickness of 6 μm, respectively.

Keywords: Bacteriochlorophyll *a*; TiO₂ film; Adsorption properties, Dye-sensitized solar cell; Photoelectric properties

1. INTRODUCTION

The application of natural dyes or pigments as photosensitizers to fabricate the cost-effectiveness and environment-friendly DSSC has been a promising research topic, this was attributed

to natural dyes' or pigments' abundance in nature, low cost of preparation, high absorption coefficients and high light-harvesting efficiency [1-2]. At present, natural dyes used in DSSC are mainly derived from plants, such as chlorophyll, anthocyanin and carotene [3-4]. Less attention was paid to the microbial pigments [5-6], especially bacteriochlorophyll *a* (BChl *a*). Natural dye-sensitized DSSCs usually perform poorly in photoelectric conversion, the main problems are that natural dyes have weak bind with TiO₂ film and poor adsorption capacity on photoanode. Prabavathy and Park *et al.* reported that photovoltaic efficiency of DSSC based on anthocyanin or gardenia yellow was depended on the adsorption quantity of natural dyes on TiO₂ film [7-8]. Nowadays, an effective pathway for enhancing photoelectric conversion efficiency of natural sensitizers is to increase the adsorption quantity of natural dyes by improving TiO₂ photoanode. It has been reported that the TiO₂ film modified with carboxylic acid [9, 10] and TiCl₄ [11-14] could improve the surface morphology of TiO₂ film and TiO₂ conduction band edge. These changes in TiO₂ film enhanced the dyes' adsorption capacity and charge transfer efficiency and blocked the charge recombination at the interface between the FTO conducting glass and electrolyte, thereby, increased the photocurrent [14-17].

A challenge in existing DSSC is the expansion of absorbance range of photoactive layers [3, 18, 19]. Therefore, the fabrication of NIR-responsive DSSC would be an especial attractive direction. BChl *a* from purple bacteria possesses high molar extinction coefficient and visible near-infrared absorption properties. Our previous studies focused on natural BChl *a* pigment and illustrated that BChl *a* could be a potential promising pigment for near-infrared responsive DSSC [20]. However, BChl *a*'s poor adsorption capacity on TiO₂ film limited its photoelectric performance. In this study, to enhance the adsorption capacity and photoelectric conversion efficiency of BChl *a*, the surface morphology of TiO₂ on the FTO substrates was improved, and the adsorption characteristic of BChl *a* on different types and thickness of TiO₂ film were systematically investigated. Meanwhile, the photoelectric properties, including conversion efficiency (η), open-circuit voltage (V_{oc}), and short-circuit current (I_{sc}) of DSSC were investigated depending on the adsorption capacity BChl *a*.

2. EXPERIMENTAL

2.1 Bacterial sources and culture conditions

Rhodospseudomonas palustris CQV97 (GenBank access number EU882154) was cultured anaerobically in modified Ormerod medium at 30°C with continuous incandescent light of 3000 lux as described in literatures [21].

2.2 Isolation and purification of natural BChl *a*

Pigments were extracted with an acetone/methanol mixture (7:2, v/v) as described previously in reference [22]. Pigment extracts were dissolved in diethyl ether and separated on silica-gel G plate using a developing mixture of petroleum ether, hexane, isopropanol, acetone and methanol (8: 0.75:

0.2: 0.8: 0.25, v/v/v/v/v). Purified BChl *a* was obtained by scraping BChl *a* band on silica-gel G plate and dissolved in anhydrous ethanol.

2.3 Surface modification of TiO₂ film

TiO₂ colloid was prepared as described in reference [23]. TiO₂ film with a thickness of about 6 μm and an area of 0.45 cm² was prepared by coating TiO₂ colloid on the fluorine-doped tin oxide (FTO) glass plate using a doctor blade technique and sintering at 450°C for 30 min. The three different types of TiO₂ film were prepared as follows: A-TiO₂ film was prepared by immersing TiO₂ film into 1.0 wt % acetic acid-ethanol solution for 12 h at room temperature and dried at 70°C. T-TiO₂ film was prepared by immersing TiO₂ film into 0.2 M TiCl₄-ethanol solution for 60 min at 70°C, rinsed with anhydrous ethanol, dried at 70°C and sintered for 30 min at 450°C. C-TiO₂ film served as untreated TiO₂ film control.

2.4 Adsorption characteristics of BChl *a* on three different types of TiO₂ film

The adsorption equilibrium experiments were used to explore the optimal adsorption time of BChl *a* and operation temperature. A-, T- and C-TiO₂ films were periodically immersed into 91.62 μg·mL⁻¹ of BChl *a* ethanol solution at 4°C and 25°C, respectively. The BChl *a*-sensitized TiO₂ films were desorbed by methanol, followed by a vacuum drying at room temperature and redissolved in ethanol. The adsorption quantity of BChl *a* was estimated by calculating the absorbance at 774 nm using a UV-vis spectrophotometer (MAPADA UV-3200PCS, China) and the extinction coefficient values of BChl *a* (65.4 g⁻¹·cm⁻¹) in ethanol.

Based on the optimal adsorption times and temperature, the adsorption capacities of different concentration BChl *a* on three types of TiO₂ films were examined by adsorption isotherm experiments. BChl *a* concentrations were set at 16.52, 30.61, 54.18, 91.62, 183.32, 435.71 and 611.63 μg·mL⁻¹, respectively.

2.5 Effect of TiO₂ film thickness on adsorption capacity of BChl *a*

The different thicknesses of TiO₂ films (A-, T- and C-TiO₂ film) with area of 0.35 cm² were prepared according to the described method in Section 2.3. They were immersed into the concentration of 91.62 μg·mL⁻¹ BChl *a* solution to achieve adsorption equilibrium. The effect of TiO₂ film thickness on the saturated adsorption quantity of BChl *a* were investigated by using the quantitative method of BChl *a* described in Section 2.4.

2.6 Fabrication and photoelectric performance of DSSC

Dye-sensitized solar cells were assembled by injecting the electrolyte (DMPII (0.3 M), I₂ (0.05 M), LiI (0.5 M), and 4-TBP (0.5 M) in acetonitrile) into the space between the different thickness of

TiO₂ film electrode (anode electrode) and a platinum electrode. The photovoltaic features of the DSSC were characterized by measuring the I–V character curves under a simulated solar light irradiation of 100 mW·cm⁻² from a 100 W Xe lamp (Shanghai Photoelectricity Device Company XQ-500W, China). The fill factor (*FF*) and photoelectric conversion efficiency (η) of the cells were calculated according to the following equations [23]:

$$FF = P_{\text{opt}} / (I_{\text{sc}} \times V_{\text{oc}}) = (I_{\text{opt}} \times V_{\text{opt}}) / (I_{\text{sc}} \times V_{\text{oc}})$$

$$\eta = P_{\text{opt}} / P_{\text{in}} = (FF \times I_{\text{sc}} \times V_{\text{oc}}) / P_{\text{in}}$$

2.7 Effects of BChl *a* concentration on photoelectric properties of DSSC

It is interesting to explore the relationship between dye concentrations and the photoelectric properties of the corresponding DSSC. The optimal TiO₂ film electrodes were immersed in different concentrations of BChl *a* solution (91.62–650.56 $\mu\text{g}\cdot\text{mL}^{-1}$) until adsorption saturation. The I–V curves of the DSSC were measured at 100 mW·cm⁻² to investigate the effect of BChl *a* concentration on photoelectric properties.

3. RESULTS AND DISCUSSION

3.1 Absorption characteristic of BChl *a*

As shown in Fig.1, the BChl *a* from strain CQV97 exhibited a strong near-infrared absorption band around 774 nm in ethanol, corresponding to its special molecular structure (the inset in Fig.1). When BChl *a* was absorbed on TiO₂ film, its absorption maximum was red-shifted to 786 nm, indicating that an interaction between BChl *a* and TiO₂ nanoparticles was happened and resulted in a change in spatial conformation of BChl *a*. After BChl *a* was desorbed from TiO₂ film, its absorption band was restored from 786 nm to 774 nm, suggesting that native structure of BChl *a* was still kept well and BChl *a* maintained good optical characteristics on TiO₂ film.

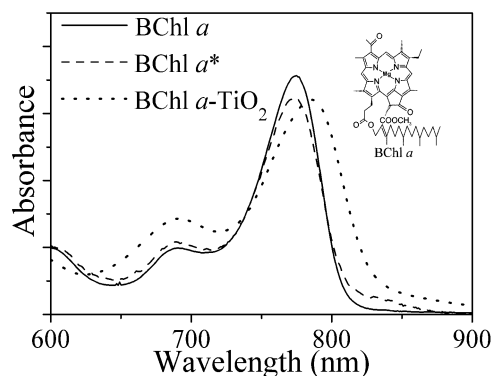


Figure 1. Absorption spectra of BChl *a* before and after adsorption on TiO₂ film electrode. BChl *a*, BChl *a* * and BChl *a*-TiO₂ represent purified BChl *a* in ethanol, desorbed BChl *a* from TiO₂ film in ethanol and absorbed BChl *a* on TiO₂ film, respectively. The inset is the structure of BChl *a*.

3.2 Adsorption properties of BChl *a* on different types of TiO₂ film

Fig.2 showed the adsorption kinetics (A) and adsorption isotherms (B) of BChl *a* on three types of TiO₂ films (A, T, C-TiO₂) at 4°C and 25°C, respectively. At 4°C (low temperature. LT), the adsorption equilibrium of A-TiO₂ film for BChl *a* was completed within 10 h, while T-TiO₂ film had the longest time of absorption equilibrium. However, at 25°C (room temperature, RT), T-TiO₂ film achieved adsorption equilibrium within 10 h, while A-TiO₂ film had the longest absorption equilibrium. The orders of BChl *a* adsorption amounts on three types of TiO₂ films at different temperature arranged: T-TiO₂-LT > A-TiO₂-RT > C-TiO₂-LT ≈ T-TiO₂-RT > C-TiO₂-RT ≈ A-TiO₂-LT. The adsorption amounts of T-TiO₂ and C-TiO₂ films for BChl *a* were increased with decreasing temperature, whereas that of A-TiO₂ film was in reverse.

The high adsorption capacity of T-TiO₂ film for BChl *a* indicated that the surface morphology of TiCl₄-treated TiO₂ film was improved, and T-TiO₂ film provided more binding sites for BChl *a*. The result was consistent with that of the previous reports [14, 15]. In addition, the effects of temperature on the adsorption capacity of T-TiO₂ and C-TiO₂ films for BChl *a* suggested that non-chemisorption dominated the BChl *a* adsorption on TiO₂ films [8].

Likewise, acetate-treated TiO₂ film (A-TiO₂) could also enhance the adsorption capacity of pigment, which was same as the previous report [9]. However, the adsorption law of A-TiO₂ film for BChl *a* was in contrasts to that of T-TiO₂ film. When TiO₂ film was treated with acetic acid, its surface increased carboxyl group [16], the main adsorption manner was changed to chemisorption, which requires activation energy to be overcome and therefore was more efficient at higher temperatures [8].

Based on the above results, the 4°C and 25 h were chosen as the adsorption temperature and time to further investigate the adsorption isotherms of BChl *a*. Fig.2B showed that the saturated adsorption amounts of BChl *a* on three types of TiO₂ films were increased with increasing dyes concentration. The T-TiO₂ film achieved the maximum saturated adsorption amount at each concentration. The adsorption isotherms process was well fitted by Langmuir isotherm model, which suggested that the adsorption of three types of TiO₂ films for BChl *a* was monolayer adsorption. This result also proved that the post-treatment of TiCl₄ increased the adsorption sites of TiO₂ film surface, and was consistent with the adsorption kinetics.

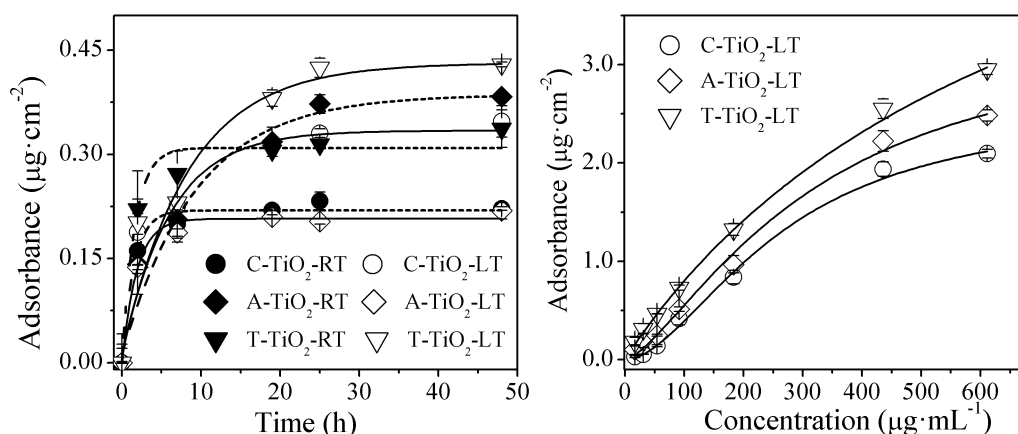


Figure 2. Adsorption kinetics (A) and adsorption isotherms (B) of BChl *a* on three types of TiO₂ films. RT and LT represent 25°C and 4°C, respectively.

3.3 Effect of TiO₂ film thickness on the adsorption amount and photoelectric properties of BChl *a*

It has been reported that the TiO₂ film thickness on photoanode has impact on adsorption amount and photoelectric characteristic of dyes [24]. Therefore, the appropriate thickness of TiO₂ film is one of the key factors in high photoelectric conversion efficiency of DSSC. As shown in Fig.3A, the saturated adsorption quantity of three types of TiO₂ films for BChl *a* were increased with increasing TiO₂ film thickness ranged from 6 to 12 μm, and T-TiO₂ film exhibited the maximal adsorption amount for BChl *a*.

To investigate the joint effect of adsorption amount and film thickness on the photoelectric performance of BChl *a*-based DSSC, T-TiO₂ films were taken as an example to examine photoelectric conversion performance due to its maximal adsorption amount for BChl *a*. As shown in Fig.3B, 3C and Table 1, the short-circuit current (*I*_{sc}) and photoelectric conversion efficiency (*η*) were increased when film thickness ranged from 6 to 10 μm, the *I*_{sc} and the *η* was increased from 0.52 to 0.68 mA·cm⁻² and from 0.23 to 0.31%, increased by 30.7% and 42.8%, respectively. The optimal TiO₂ film thickness was 10 μm. Film thickness had less effect on open-circuit voltage (*V*_{oc}) and filled factor (*FF*). The similar results were observed by Ito *et al.* [25] and Baglio *et al.* [26].

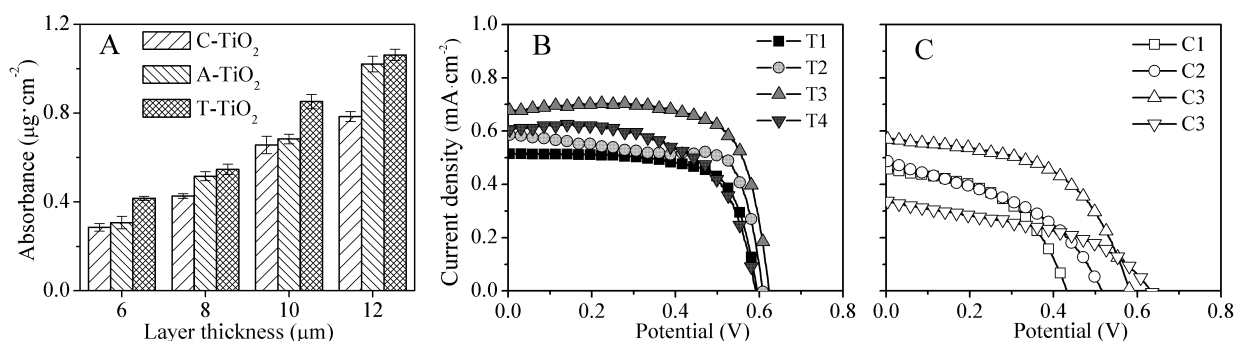


Figure 3. The adsorbance of BChl *a* on different thickness films (A) and the I-V curves of DSSC with T-TiO₂ film (B) and C-TiO₂ film (C). T1 ~ T4 represents the T-TiO₂ films thickness of 6, 8, 10, 12 μm, respectively. C1 ~ C4 represents the C-TiO₂ films thickness of 6, 8, 10, 12 μm, respectively.

Table 1. Photoelectric performance parameters of DSSC depending on different thickness TiO₂ films sensitized by BChl *a*.

Samples	<i>I</i> _{sc} (mA·cm ⁻²)	<i>V</i> _{oc} (V)	FF (%)	<i>η</i> (%)
T1	0.52	0.59	70.7	0.23
T2	0.59	0.61	72.1	0.26
T3	0.68	0.62	70.1	0.31
T4	0.61	0.60	62.5	0.22
C1	0.45	0.43	51.6	0.10
C2	0.48	0.51	49.1	0.12
C3	0.57	0.58	54.4	0.18
C4	0.34	0.63	42.0	0.09

For the better understanding of the reason why T-TiO₂ films had increased photocurrent and conversion efficiency, the dark current-voltage was investigated. Fig.4 showed the dark I-V characteristics of two types of TiO₂ film electrodes with absorbed BChl *a*. As shown in Fig.4, the suppression of dark current was depended on film thickness. When film thickness of C-TiO₂ film ranged from 6 to 10 μm, the V_{oc} corresponding to the beginning of dark current was increased with increasing film thickness, indicating that the dark current was suppressed. When film thickness was 12 μm, the suppression of dark current was alleviated. It suggested that thicker TiO₂ film prolonged electronic transmission distance, which increased the recombination of electrons in TiO₂ semiconductor film.

Compared with C-TiO₂ film, T-TiO₂ film could effectively suppress the dark current, and its open-circuit voltage was increased by several hundred millivolts (30 ~ 500 mV). A similar result was observed in previous reports [27, 28]. As far as we know, one reason for dark reaction occurring is the recombination of electrons in TiO₂ semiconductor conduction band with I₃⁻ from electrolyte. Thus, in order to prevent from charge recombination, the contact between the electrons and I₃⁻ should be avoided as far as possible, or the reduction process of I₃⁻ on the Pt electrode should be promoted as far as possible.

The TiCl₄ treatment led to grow a density layer of TiO₂ particles as a blocking layer on the surface of TiO₂ film, which improved dye adsorption amount and electron transport efficiency, and reduced the charge recombination rate in semiconductor conduction band. Meanwhile, the growth of TiO₂ particles resulted in enhancing the connection between conductive glass substrates and the nanocrystalline TiO₂, improving the charge injection into the TiO₂ and the photoelectric conversion efficiency of DSSC. This result was consistent with the result of I-V curves above.

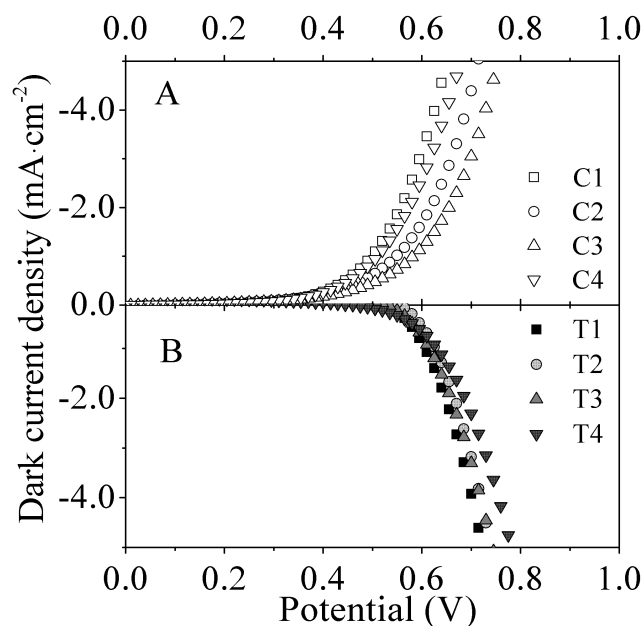


Figure 4. The dark I-V curves of DSSC with C-TiO₂ film (A) and T-TiO₂ film (B). T1 ~ T4 represents the T-TiO₂ films thickness of 6, 8, 10, 12 μm, respectively. C1 ~ C4 represents the C-TiO₂ films thickness of 6, 8, 10, 12 μm, respectively.

3.4 Effect of BChl *a* concentration on photoelectric properties of DSSC

The data of the adsorption isotherms showed that the dye adsorption amounts on TiO₂ film were related to the initial concentration of dye. The exploration of the effect of BChl *a* concentration on the performance of DSSC was helpful to obtain an optimal operation parameter. Fig.5A and 5B showed that the both I_{sc} and η of DSSC were increased with increasing concentrations of BChl *a* ranged from 91.62 ~ 483.67 $\mu\text{g/ml}$, V_{oc} was less affected by BChl *a* concentrations (Fig. 5C). The optimum concentration of natural BChl *a* sensitizer was about 480 $\mu\text{g}\cdot\text{mL}^{-1}$, and the maximum I_{sc} and η was 3.51 $\text{mA}\cdot\text{cm}^{-2}$ and 1.67%, respectively (Fig. 5D). When the dye concentration was beyond the optimal concentration, BChl *a* molecules tended to aggregation, which may lead to the singlet and triplet quenching reaction of dye molecules each other, the electron transfer between the excited BChl *a* and TiO₂ film was reduced.

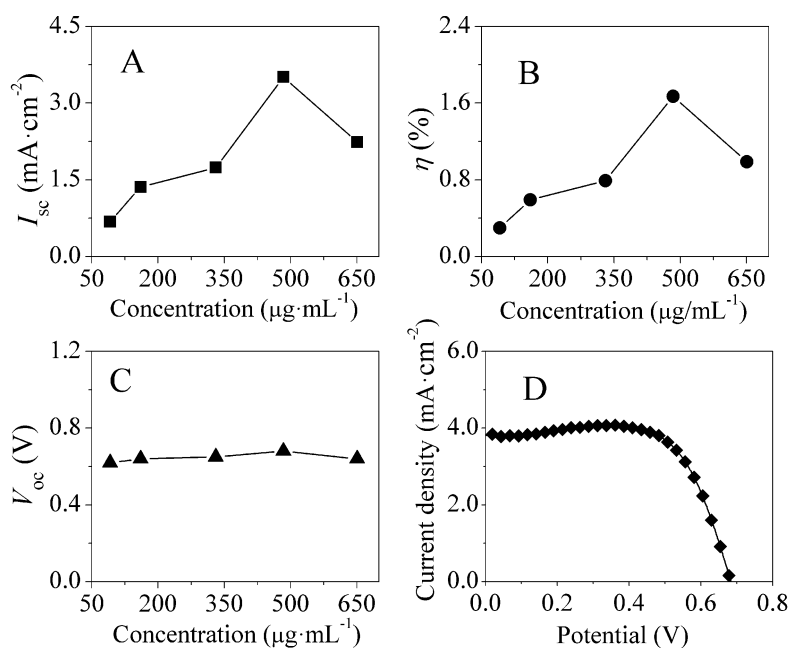


Figure 5. Variation of short I_{sc} (A), V_{oc} (B) and η (C) as a function of BChl *a* concentration, and the I-V curve of DSSC at the concentration of 483.67 $\mu\text{g}\cdot\text{mL}^{-1}$ BChl *a* (D).

4. CONCLUSION

Adsorption properties revealed that the adsorption of BChl *a* onto TiO₂ film depended on the temperature, surface morphology, film thickness and dye concentrations. Compared with acetic acid-treated and non-treated TiO₂ (A-TiO₂ and C-TiO₂) film, the TiCl₄-treated TiO₂ (T-TiO₂) film could reach adsorption equilibrium rapidly and had the maximum adsorption amount for BChl *a* at 4°C, which are 1.2 times higher than that of two other types of TiO₂ film.

The adsorption amounts of three types of TiO₂ films were increased with increasing thickness and dye concentration. However, the short-circuit current and photoelectric conversion efficiency were

first increased and then decreased with the increasing of thickness and concentration of BChl *a*. The optimal film thickness and BChl *a* concentration were 10 μm and 480 $\mu\text{g}\cdot\text{ml}^{-1}$, respectively. TiCl_4 treatment increased the adsorption sites and adsorption capacity of TiO_2 film, and enhanced the photoelectric properties of DSSC, such as the photocurrent and photoelectric conversion efficiency were eight times and fifteen times higher than those of untreated TiO_2 films with thickness of 6 μm , respectively. Meanwhile, the TiCl_4 treatment effectively inhibited the charge recombination rate in semiconductor conduction band. In this study, the DSSC based on natural BChl *a* and modified TiO_2 film achieved an I_{sc} of 3.51 $\text{mA}\cdot\text{cm}^{-2}$ and a η of 1.67% under an incident light intensity of 100 $\text{mW}\cdot\text{cm}^{-2}$. The systematic studies of adsorption properties of natural sensitizers on TiO_2 film could be give the important signification of enhancing the adsorption amount and photoelectric property of natural sensitizers.

ACKNOWLEDGMENTS

This work has been supported by National Marine Public Industry Research (No.201505026), the National Natural Science Foundation of China (31270106), by Natural Science Foundation of Fujian Province (No. 2015J01137, 2018J0149), by Subsidized Project for Cultivating Postgraduates' Innovative Ability in Scientific Research of Huaqiao University.

References

1. P. Sanjay, K. Deepa, J. Madhavan, S. Senthil, *Mater. Lett*, 219 (2018) 158.
2. M. Shahid, I. Shahidul, F. Mohammad, *J Clean Prod*, 53 (2013) 310.
3. M.R. Narayan, *Renew Sust Energ Rev*, 16 (2012) 208.
4. Y. Koyama, Y. Kakitani, H. Nagae, *Molecules*, 17 (2012) 2188.
5. S. Ito, T. Saitou, H. Imahori, H. Uehara, N. Hasegawa, *Energ Environ Sci*, 3 (2010) 905.
6. R. Tange, K. Inai, T. Sagawa, S. Yoshikawa, *J Mater Res*, 26 (2011) 306.
7. N. Prabavathy, S. Shalini, R. Balasundaraprabhu, D. Velauthapillai, S. Prasanna, G. Balaji, N. Muthukumarasamy, *Int J Energ Res*, 42 (2018) 790.
8. K.H. Park, T.Y. Kim, J.Y. Park, E.M. Jin, S.H. Yim, D.Y. Choi, J.W. Lee, *Dyes Pigments*, 96 (2013) 595.
9. H.G. Bang, J.K. Chung, R.Y. Jung, S.Y. Park, *Ceram Int*, 38 (2012) S511.
10. H. Jeong, Y. Lee, Y. Kim, M. Kang, *Korean J Chem Eng*, 27 (2010) 1462.
11. M.D. Ye, D.J. Zheng, M.Q. Lv, C. Chen, C.J. Lin, Z.Q. Lin, *Adv Mater*, 25 (2013) 3039.
12. A. Sedghi, H.N. Miankushki, *Japn J Appl Phys*, 52 (2013) UNSP 075002.
13. S.N. Sadikin, M.Y.A. Rahman, A.A. Umar, M.M. Salleh, *Int J Electrochem Sc*, 12 (2017) 5529.
14. J.S. Lee, K.H. Kim, C.S. Kim, H. Choi, *J Nanosci Nanotechno*, 16 (2016) 10526.
15. P.M. Sommeling, B.C. O'Regan, R.R. Haswell, H.J.P. Smit, N.J. Bakker, J.J.T. Smits, J. M. Kroon, J.A.M. van Roosmalen, *J Phys Chem B*, 110 (2006) 19191.
16. M. Murayama, T. Mori, *Japn J Appl Phys*, 45 (2006) 542.
17. C. Sandquist, J.L. McHale, *J Photoch Photobio A*, 221 (2011) 90.
18. J.H. Wu, G.T. Yue, Y.M. Xiao, J.M. Lin, M.L. Huang, Z. Lan, Q.W. Tang, Y.F. Huang, L.Q. Fan, S. Yin, Sato T, *Sci Rep*, 3 (2013) 1283.
19. Q.M. Fu, C.G. Zhao, S.P. Yang, J.H. Wu, *Mater Lett*, 129 (2014) 195.
20. Q.M. Fu, C.G. Zhao, S.P. Yang, *CIESC Journal*, 65 (2014) 3202.
21. L. Zhao, C.G. Zhao, D.X. Han, S.P. Yang, S.H. Chen, C.P. Yu, *Biotechnol Lett*, 33 (2011) 2135.
22. M.Q. Zhuo, C.G. Zhao, Q.R. Cheng, S.P. Yang, Y.B. Qu, *Acta microbiologica Sinica*, 52 (2012)

760.

23. J.H. Wu, J.L. Wang, J.M. Lin, Z. Lan, Q.W. Tang, M.L. Huang, *Adv Energy Mater*, 2 (2012) 78.
24. J. Xu, G.X. Wang, J.J. Fan, B.S. Liu, S.W. Cao, J.G. Yu, *J Power Sources*, 274 (2015) 77.
25. S. Ito, T.N. Murakami, P. Comte, P. Liska, C. Gratzel, M.K. Nazeeruddin, M. Gratzel, *Thin Solid Films*, 516 (2008) 4613.
26. V. Baglio, M. Girolamo, V. Antonucci, A. Aricò, *Int J Electrochem Sc*, 6 (2011) 3375.
27. S. Ito, P. Liska, P. Comte, R.L. Charvet, P. Pechy, U. Bach, L. Schmidt-Mende, S.M. Zakeeruddin, A. Kay, M.K. Nazeeruddin, M. Gratzel, *Chem Commun*, 34 (2005) 4351.
28. D.P. Chen, X.D. Zhang, C.C. Wei, C.C. Liu, Y. Zhao., *Acta Physico-Chimica Sinica*, 27 (2011) 425.

© 2018 The Authors. Published by ESG (www.electrochemsci.org). This article is an open access article distributed under the terms and conditions of the Creative Commons Attribution license (<http://creativecommons.org/licenses/by/4.0/>).